

# Synthesis, Crystal Structure, and Magnetic Property of Delithiated $\text{Li}_x\text{MnO}_2$ ( $x < 0.1$ ) Single Crystals: A Novel Disordered Rocksalt-Type Manganese Dioxide

Junji Akimoto,\* Yasuhiko Takahashi, Yoshito Gotoh, and Kenji Kawaguchi

National Institute of Advanced Industrial Science and Technology (AIST), 1-1-1 Higashi, Tsukuba 305-8565, Japan

Kaoru Dokko and Isamu Uchida

Department of Applied Chemistry, Graduate School of Engineering, Tohoku University, Aramaki-Aoba 07, Aoba-ku, Sendai 980-8579, Japan

Received March 12, 2003. Revised Manuscript Received May 13, 2003

Single crystals of the chemically and electrochemically delithiated  $\text{Li}_x\text{MnO}_2$  ( $x < 0.1$ ) have been successfully synthesized from the parent orthorhombic  $\text{LiMnO}_2$  single crystals. A single-crystal X-ray diffraction study revealed that the average structure of  $\text{Li}_x\text{MnO}_2$  was the disordered rocksalt-type with the space group  $Fm\bar{3}m$ , and the lattice parameter  $a = 4.095(3)$  Å. Some additional spots indicating the superlattice structure and diffuse scattering could be observed in the X-ray precession photographs. The mechanism of the structural transformation from the parent orthorhombic  $\text{LiMnO}_2$  to the delithiated cubic  $\text{Li}_x\text{MnO}_2$  was well explained by the manganese ion migration accompanied with  $\text{Li}^+$  extraction. The magnetic properties of the chemically delithiated  $\text{Li}_x\text{MnO}_2$  are compared with those of the parent  $\text{LiMnO}_2$ . The extracted Curie constant in  $\text{Li}_x\text{MnO}_2$  is consistent with the residual lithium content found analytically, as in the case of  $\lambda\text{-MnO}_2$ .

## Introduction

Layered lithium manganese oxides have attracted intense research interest as prospective cathode materials in secondary lithium batteries not only because of the low cost and low toxicity of manganese, but also because of their high theoretical capacities.<sup>1–4</sup>  $\text{LiMnO}_2$  is known to exist in two ordered rocksalt-type structures with orthorhombic and monoclinic symmetry, respectively. Orthorhombic  $\text{LiMnO}_2$  has a zigzag layered  $\beta\text{-NaMnO}_2$  type structure with the space group of  $Pmmn$ , as shown in Figure 1. The detailed crystal structure of this compound was deduced first from powder, and later from single-crystal, X-ray diffraction data.<sup>5–7</sup> It is experimentally well-known that the structure of orthorhombic  $\text{LiMnO}_2$  cathode transforms gradually and irreversibly into a spinel-type structure during several discharge–charge cycles.<sup>2,3</sup> For practical reasons, such a structural change of electrodes is generally unfavorable, but in this case, the electrochemically generated spinel electrodes show significantly better

and more stable characteristics of the charge–discharge cycles than the regular spinel-type  $\text{LiMn}_2\text{O}_4$  electrodes.

Recently, Tang et al.<sup>8</sup> reported a structural-transformation model of orthorhombic  $\text{LiMnO}_2$  to spinel-type  $\text{LiMn}_2\text{O}_4$  accompanied by the  $\text{Li}^+$  extraction. In contrast, Chiang et al.<sup>9</sup> reported the role of cation disorder and transformation microstructures on electrochemical performance examined theoretically and experimentally. They predicted an intermediate structure with  $Fm\bar{3}m$  space group between the parent orthorhombic structure with  $Pmmn$  space group and the spinel-type structure with  $Fd\bar{3}m$  space group, from the viewpoint of crystallographic considerations. However, such an intermediate structure could not be obtained experimentally as an average structure. To clarify the true crystal symmetry, precise crystal structure, and mechanism of the structure change in this intercalation system, the single-crystal X-ray diffraction method has been highly desired, as in the recent studies of the spinel-type  $\text{Li}_{1-x}\text{Mn}_2\text{O}_4$ .<sup>10–15</sup>

\* Corresponding author. E-mail: j.akimoto@aist.go.jp. Fax: +81-29-861-4803.

- (1) Armstrong, A. R.; Bruce, P. G. *Nature* **1996**, *381*, 499.
- (2) Ohzuku, T.; Ueda, A.; Hirai, T. *Chem. Express* **1992**, *7*, 193.
- (3) Gummow, R. J.; Liles, D. C.; Thackeray, M. M. *Mater. Res. Bull.* **1993**, *28*, 1249.
- (4) Shao-Horn, Y.; Hackney, S. A.; Armstrong, A. R.; Bruce, P. G.; Gitzendanner, R.; Johnson, C. S.; Thackeray, M. M. *J. Electrochem. Soc.* **1999**, *146*, 2404.
- (5) Johnston, W. D.; Heikes, R. R. *J. Am. Chem. Soc.* **1956**, *78*, 3255.
- (6) Dittrich, G.; Hoppe, R. *Z. Anorg. Allg. Chem.* **1969**, *368*, 262.
- (7) Hoppe, R.; Brachtel, G.; Jansen, M. Z. *Anorg. Allg. Chem.* **1975**, *417*, 1.

(8) Tang, W.; Kanoh, H.; Ooi, K. *J. Solid State Chem.* **1999**, *142*, 19.

(9) Chiang, Y.-M.; Wang, H.; Jang, Y.-I. *Chem. Mater.* **2001**, *13*, 53.

(10) Akimoto, J.; Takahashi, Y.; Gotoh, Y.; Mizuta, S. *Chem. Mater.* **2000**, *12*, 3246.

(11) Björk, H.; Gustafsson, T.; Thomas, J. O. *Electrochim. Commun.* **2001**, *3*, 187.

(12) Tang, W.; Yang, X.; Kanoh, H.; Ooi, K. *Chem. Lett.* **2001**, 524.

(13) Akimoto, J.; Takahashi, Y.; Gotoh, Y.; Mizuta, S. *J. Cryst. Growth* **2001**, *229*, 405.

(14) Monge, M. A.; Amarilla, J. M.; Gutiérrez-Puebla, E.; Campa, J. A.; Rasines, I. *ChemPhysChem* **2002**, *3*, 367.

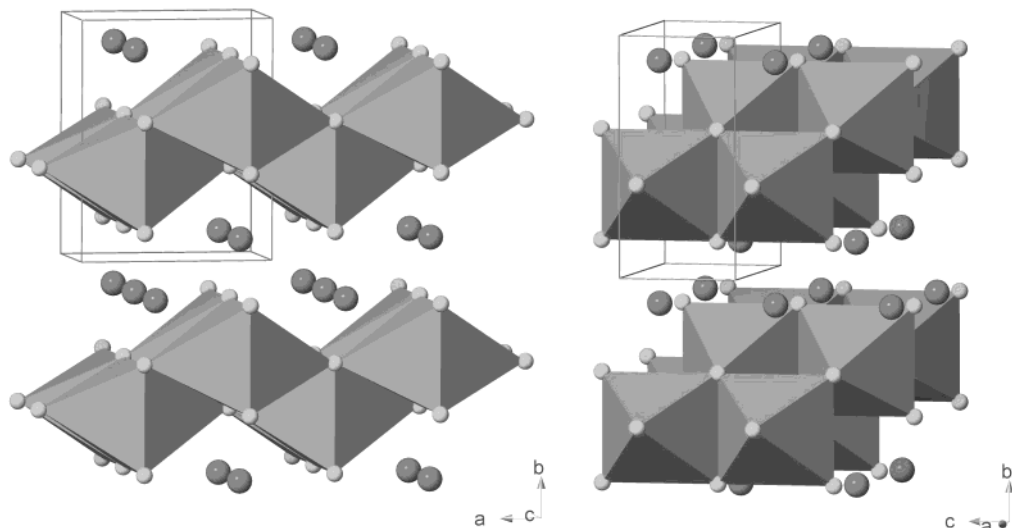


**Figure 1.** Crystal structure of orthorhombic  $\text{LiMnO}_2$ .

The present paper has three main objectives. First, we prepare the electrochemically delithiated  $\text{Li}_x\text{MnO}_2$  ( $x < 0.1$ ) single crystals and determine the precise crystal structure by the single-crystal X-ray diffraction method. Second, we explain the mechanism of structural transformation by the manganese ion migration accompanied with  $\text{Li}^+$  extraction. Finally, we demonstrate the magnetic property of the novel disordered rocksalt-type manganese dioxide compound obtained by the  $\text{Li}^+$  extraction from the parent orthorhombic  $\text{LiMnO}_2$  single crystals.

## Experimental Section

**Single-Crystal Synthesis.** Single crystals of the orthorhombic  $\text{LiMnO}_2$  were grown by a flux method, as mentioned previously.<sup>16</sup> The as-prepared  $\text{LiMnO}_2$  powder (Nippon Chemical Industrial Co., Ltd., Japan) was mixed with  $\text{LiCl}$  (99.9%) as a flux material in the nominal weight ratio of  $\text{LiMnO}_2/\text{LiCl} = 1:10$ . The flux growth was conducted in a vertical resistance furnace. The mixture was heated to 1273 K for 10 h in a sealed Pt tube, gradually cooled to 873 K, and then cooled naturally. The produced single crystals were easily separated from the frozen  $\text{LiCl}$  flux by rinsing the Pt tube in water for several hours.

**Chemical Analysis.** Chemical analyses of selected single-crystal specimens were carried out by SEM-EDX (JEOL JSM-5400). The chemical formulas of the samples were analyzed by inductively coupled plasma (ICP) spectroscopy using the pulverized single crystals (about 6 mg).

**Electrochemical Delithiation.** The controlled extraction of lithium from a piece of single crystal was achieved by electrochemical means using a microelectrode-based system.<sup>17–20</sup> A selected  $\text{LiMnO}_2$  crystal ( $0.15 \times 0.03 \times 0.02 \text{ mm}^3$ ) was placed on a glass paper soaked in 1 M  $\text{LiClO}_4$ /propylene carbonate (PC) + ethylene carbonate (EC) (1:1 vol) solution (Li-ion battery grade, Mitsubishi Kagaku Co.). A Pt–Rh fine filament (25  $\mu\text{m}$  diam) was coated with a thin film of Teflon (Cytop, Asahi Glass), and was then cut to give a micro-disk electrode. The prepared microelectrode was held with x-y-z microposi-

tioner (Shimadzu MMS-77) and brought into contact with the  $\text{LiMnO}_2$  crystal by handling the positioner under observation with a stereomicroscope (Nikon SMZ-U). The electrode potential was measured and controlled against a Li foil reference electrode with a potentiostat (Hokuto Denko HA-150). All the electrochemical experiments were conducted in a small drybox filled with air purified by a column (Balston 75-20, 203 K dew point).

The electrode potential was stepped from the open circuit potential (OCP, about 3.2 V) of  $\text{LiMnO}_2$  to a desired value, such as 4.50 V vs Li. After the overnight electrolysis, the potentiostat was switched back to the OCP-measuring mode. We checked the completion of the extraction reaction with the stability of the regulated OCP, the value of which was 4.10 V vs Li. The obtained  $\text{Li}_x\text{MnO}_2$  crystal was rinsed carefully with pure PC, and then supplied to the single-crystal X-ray diffraction analysis.

**Chemical Delithiation.** The  $\text{Li}_x\text{MnO}_2$  single crystals were also prepared by a combined Li-ion extraction/chemical oxidation process. Selected  $\text{LiMnO}_2$  single crystals were placed in 1 M HCl solution for several hours. No stirring or heating was performed. The obtained  $\text{Li}_x\text{MnO}_2$  crystals were washed carefully with ethanol, and then supplied to chemical analysis, powder X-ray diffraction, and magnetic measurements.

**Single-Crystal X-ray Diffraction.** Crystals were examined with an X-ray precession camera ( $\text{MoK}\alpha$  radiation filtered by Zr foil) to check on the crystal quality and to determine the lattice parameters, systematic extinctions, and possible superstructures. Integrated intensity data for the as-grown  $\text{LiMnO}_2$  and the electrochemically delithiated  $\text{Li}_x\text{MnO}_2$  single crystals were collected in the  $2\theta-\omega$  scan mode at a scan rate of 1.0°/min at 296 K on a Rigaku AFC-5S four-circle diffractometer (operating conditions 45 kV, 35 mA) using graphite-monochromatized  $\text{MoK}\alpha$  radiation ( $\lambda = 0.71073 \text{ \AA}$ ), and reduced to structure factors after due corrections for absorption and Lorentz and polarization effects. The lattice parameters of these compounds were determined by least-squares refinement using  $2\theta$  values of 25 strong reflections in the range 20–30° and  $\text{MoK}\alpha$  ( $\lambda = 0.71073 \text{ \AA}$ ) on the four-circle diffractometer.

**Powder X-ray Diffraction.** The X-ray powder diffraction profiles were measured using a Rigaku RINT2550 diffractometer (operating conditions 40 kV, 200 mA) with  $\text{CuK}\alpha$  radiation equipped with a curved graphite monochromator. The  $d$  spacing measurements were performed at  $2.0^\circ (2\theta) \text{ min}^{-1}$  in the range of  $10^\circ < 2\theta < 80^\circ$  using powdered single crystals. Lattice parameters were calculated by a least-squares method.

**Magnetic Measurements.** The temperature dependence of the magnetic susceptibility was measured with a SQUID magnetometer (Quantum Design, MPMS) in a temperature

(15) Takahashi, Y.; Akimoto, J.; Gotoh, Y.; Dokko, K.; Nishizawa, M.; Uchida, I. *J. Phys. Soc. Jpn.* **2003**, *72*, 1483.

(16) Strobel, P.; Levy, J.-P.; Joubert, J.-C. *J. Cryst. Growth* **1984**, *66*, 257.

(17) Uchida, I.; Fujiyoshi, H.; Waki, S. *J. Power Sources* **1997**, *68*, 139.

(18) Nishizawa, M.; Uchida, I. *Electrochim. Acta* **1999**, *44*, 3629.

(19) Nishizawa, M.; Koshika, H.; Hashitani, R.; Itoh, T.; Abe, T.; Uchida, I. *J. Phys. Chem. B* **1999**, *103*, 4933.

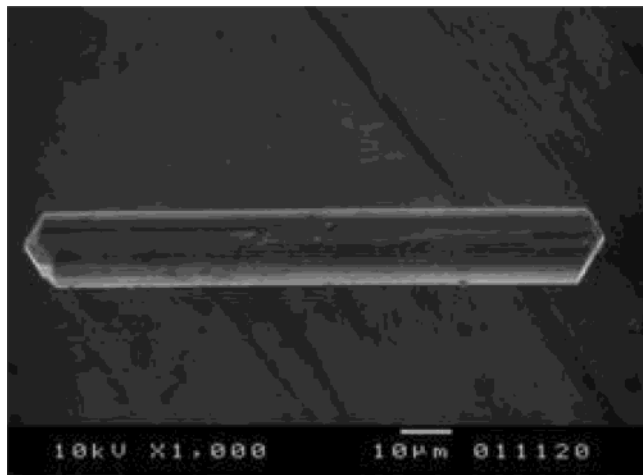


**Figure 2.** SEM photograph of as-grown  $\text{LiMnO}_2$  single crystal.

range from 4.5 to 300 K at applied fields of 10, 20, and 100 Oe. Diamagnetic corrections for magnetic susceptibilities were taken into account.

### Results and Discussion

**LiMnO<sub>2</sub>.** Black, needlelike  $\text{LiMnO}_2$  single crystals of about  $0.15 \times 0.03 \times 0.02 \text{ mm}^3$  in average were obtained, as shown in Figure 2. EDX analysis showed that the crystals were free from platinum contamination from the vessel. The chemical formula, analyzed by ICP, was  $\text{Li}_{1.0}\text{Mn}_{1.0}\text{O}_2$ , which is consistent with the result of the present structure refinement.

Precession photographs indicate the as-grown  $\text{LiMnO}_2$  belongs to the orthorhombic system with the space group  $Pmnm$ , as in the previous work.<sup>7</sup> Figure 3 shows the  $\{h0l\}^*$  and  $\{0kl\}^*$  precession photographs of the  $\text{LiMnO}_2$  single crystal, taken at room temperature. No additional spots indicating the ordered structure and diffuse scattering could be observed in these photographs. The lattice parameters for the as-grown  $\text{LiMnO}_2$  were identical with those in the previous report.<sup>7,16</sup>

The structure refinement for orthorhombic  $\text{LiMnO}_2$  was carried out with the atomic coordinates reported in the literature.<sup>7</sup> The converged final  $R$  and  $wR$  values and other experimental and crystallographic data are summarized in Table 1. Difference Fourier syntheses using the final atomic parameters showed no significant residual peaks. The final atomic coordinates and displacement parameters are given in Table 2. All calculations were carried out using the Xtal3.4 package program.<sup>21</sup> The refined structural parameters are in excellent agreement with those in the previous reports for  $\text{LiMnO}_2$ .<sup>7</sup>

Magnetic susceptibility was measured as a function of temperature at fixed fields using the present  $\text{LiMnO}_2$  single-crystal samples. Figure 4 shows a typical temperature dependence from 5 to 300 K at 100 Oe. The open and filled marks correspond to measurements on field cooling and on heating after zero-field cooling, respectively. The history dependence of temperature

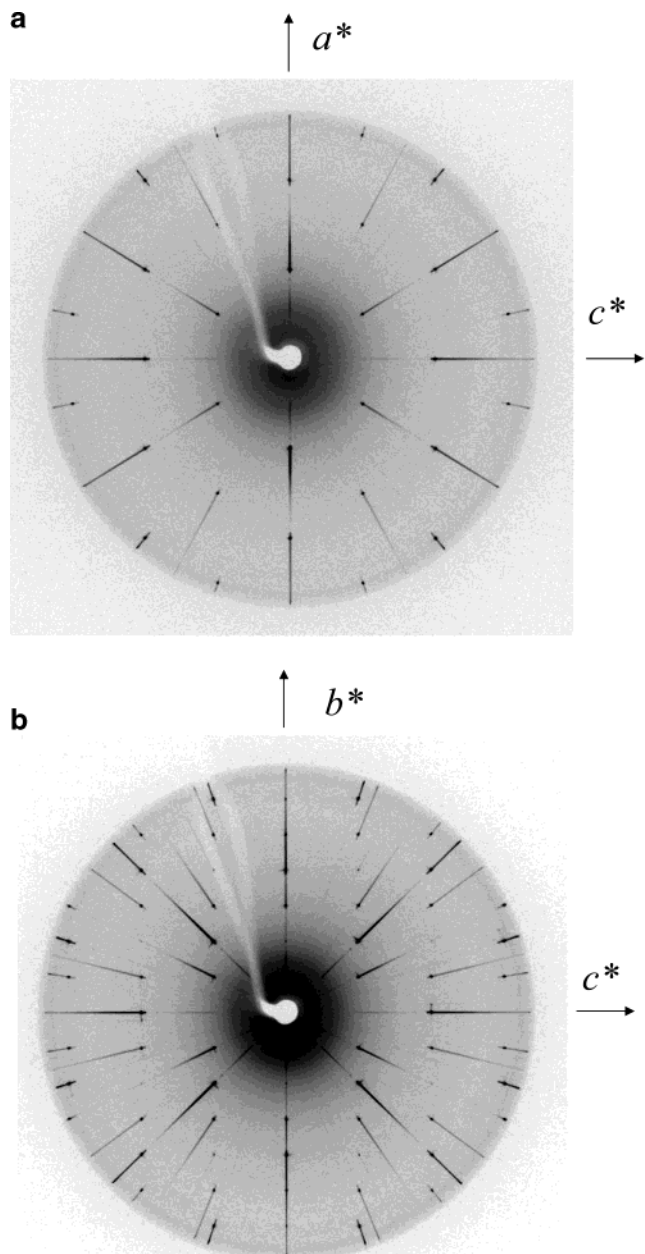


**Figure 3.** (a)  $\{h0l\}^*$  and (b)  $\{0kl\}^*$  precession photographs of as-grown orthorhombic  $\text{LiMnO}_2$  single crystal. MoK $\alpha$  radiation filtered by Zr foil was used.

versus  $M/H$  maximum below 50 K was clearly observed. Similar features were observed previously in the  $\text{LiMnO}_2$  polycrystalline sample.<sup>22</sup>

From the results of the present structural and magnetic characterization, we confirmed that the present single-crystal sample had a stoichiometric  $\text{LiMnO}_2$  chemical composition.

**$\text{Li}_x\text{MnO}_2$  ( $x < 0.1$ ).** Figure 5 shows a SEM photograph of the electrochemically delithiated  $\text{Li}_x\text{MnO}_2$  single crystal. Compared with that of the parent  $\text{LiMnO}_2$ , the crystal becomes fragile, and there are many surface grooves parallel to the needle direction. The color of the crystals changed from black to brown by  $\text{Li}^+$  extraction.

(20) Dokko, K.; Nishizawa, M.; Mohamedi, M.; Umeda, M.; Uchida, I.; Akimoto, J.; Takahashi, Y.; Gotoh, Y.; Mizuta, S. *Electrochim. Solid State Lett.* **2001**, 4, A151.

(21) Hall, S. R.; King, G. S. D.; Stewart, J. M., Eds. *Xtal3.4 User's Manual*. University of Western Australia: Lamb, Perth, 1995.

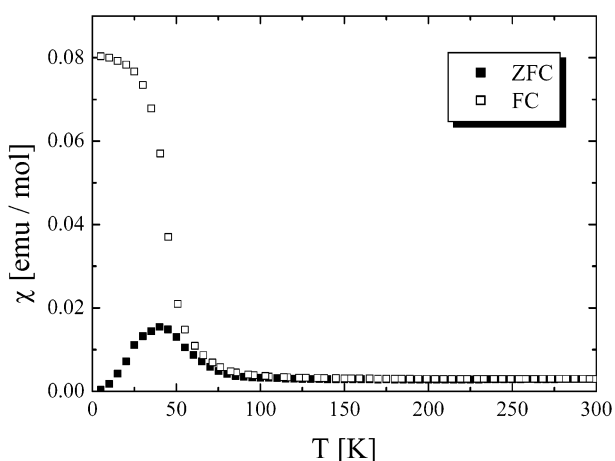
(22) Greedan, J. E.; Raju, N. P.; Davidson, I. J. *J. Solid State Chem.* **1997**, 128, 209.

**Table 1. Experimental and Crystallographic Data for Orthorhombic  $\text{LiMnO}_2$** 

formula	$\text{LiMnO}_2$
crystal system	orthorhombic
space group	$Pmmn$ (no. 59)
lattice parameters	
$a$ (Å)	4.574(1)
$b$ (Å)	5.752(1)
$c$ (Å)	2.808(1)
$V$ (Å <sup>3</sup> )	73.86(3)
crystal size (mm)	0.13 × 0.03 × 0.03
temperature (K)	296
scan type	$2\theta - \omega$
scan speed (°/min)	1.0
maximum $2\theta$ (°)	70
absorption correction	Gaussian integration
transmission factors	
min.	0.760
max.	0.795
measured reflections	978
$R_{\text{int}}$ (%)	1.06
independent observed reflections	207
number of variables	18
$R$ (%)	1.30
$wR$ [ $w = 1/\sigma^2 F$ ] (%)	1.57

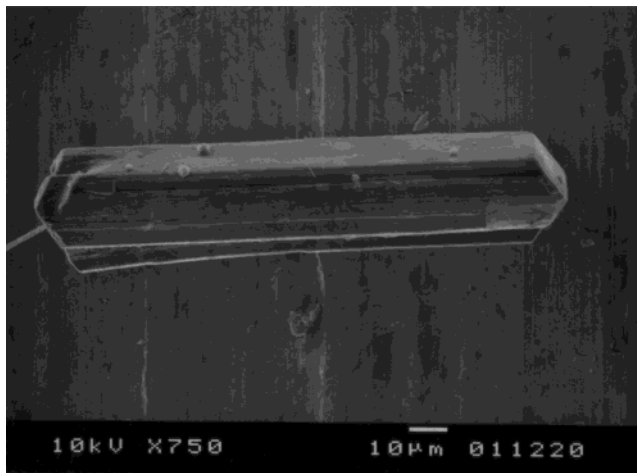
**Table 2. Structural Parameters for Orthorhombic  $\text{LiMnO}_2$** 

atom	$x$	$y$	$z$	$U_{\text{eq}}$ (Å <sup>2</sup> )
Li	1/4	0.1161(7)	1/4	0.010(2)
Mn	1/4	0.63477(6)	1/4	0.0043(2)
O1	3/4	0.1423(3)	1/4	0.0068(7)
O2	3/4	0.5993(3)	1/4	0.0058(7)

**Figure 4.** Temperature dependence of the magnetic susceptibility for as-grown  $\text{LiMnO}_2$  single crystals measured at  $H = 100$  Oe after zero-field cooling (filled symbols) and on-field cooling (open symbols).

The chemical formula of the electrochemically delithiated single crystal was roughly estimated (from the OCP value) to be  $\text{Li}_{0.1}\text{MnO}_2$ . The chemical composition of the chemically delithiated crystals, analyzed by ICP, was  $\text{Li}_{0.06}\text{Mn}_{1.0}\text{O}_2$ . The value is well consistent with that obtained by the electrochemical delithiation. The chemical formula of both the electrochemically and chemically delithiated compounds is hereafter denoted as  $\text{Li}_x\text{MnO}_2$ , where the lithium content,  $x$ , is less than 0.1.

Precession photographs indicate the average structure of the electrochemically delithiated  $\text{Li}_x\text{MnO}_2$  belongs to the cubic system with the space group  $Fm\bar{3}m$ . Figure 6 shows the  $\{hk0\}^*$  and  $\{hh\}^*$  precession photographs of the electrochemically delithiated  $\text{Li}_x\text{MnO}_2$  single crystal, taken at room temperature. Some additional

**Figure 5.** SEM photograph of electrochemically delithiated  $\text{Li}_{0.1}\text{MnO}_2$  single crystal.**Table 3. Experimental and Crystallographic Data for Cubic  $\text{Li}_x\text{MnO}_2$** 

structural formula	$\text{MnO}_2$
crystal system	cubic
space group	$Fm\bar{3}m$ (no. 225)
lattice parameters	
$a$ (Å)	4.095(3)
$V$ (Å <sup>3</sup> )	68.67(15)
crystal size (mm)	0.18 × 0.02 × 0.02
temperature (K)	296
scan type	$2\theta - \omega$
scan speed (°/min)	1.0
maximum $2\theta$ (°)	70
absorption correction	Gaussian integration
transmission factors	
min.	0.532
max.	0.845
measured reflections	55
$R_{\text{int}}$ (%)	6.2
independent observed reflections	18
number of variables	4
$R$ (%)	6.4
$wR$ [ $w = 1/\sigma^2 F$ ] (%)	6.7

spots indicating the superlattice structure and diffuse scattering could be observed in these photographs (Figure 7). This fact suggests the ordered local structure or short-range ordering in the single crystal specimen, as previously observed by electron diffraction study.<sup>9</sup> However, these reflections were very weak in intensity compared with the main Bragg reflections. Therefore, we can describe the average structure as disordered rocksalt-type. The lattice parameter for the cubic rocksalt-type structure model was determined to be  $a = 4.095$  (3) Å using a four-circle diffractometer. The value is considerably different from those in the disordered rocksalt-type  $\text{MnO}$  ( $a = 4.446$ (1) Å) and the spinel-type  $\lambda\text{-MnO}_2$  ( $a = 4.02 \times 2$  Å).<sup>23,24</sup>

The structure refinement for the electrochemically delithiated  $\text{Li}_x\text{MnO}_2$  was carried out with the disordered rocksalt-type atomic coordinates and the space group  $Fm\bar{3}m$ . The converged final  $R$  and  $wR$  values and other experimental and crystallographic data are summarized in Table 3. Difference Fourier syntheses using the final atomic parameters showed no significant residual peaks,

(23) Sasaki, S.; Fujino, K.; Takéuchi, Y.; Sadanaga, R. *Acta Crystallogr., Sect. A* **1980**, *36*, 904.

(24) Greidan, J. E.; Raju, N. P.; Wills, A. S.; Morin, C.; Shaw, S. M. *Chem. Mater.* **1998**, *10*, 3058.

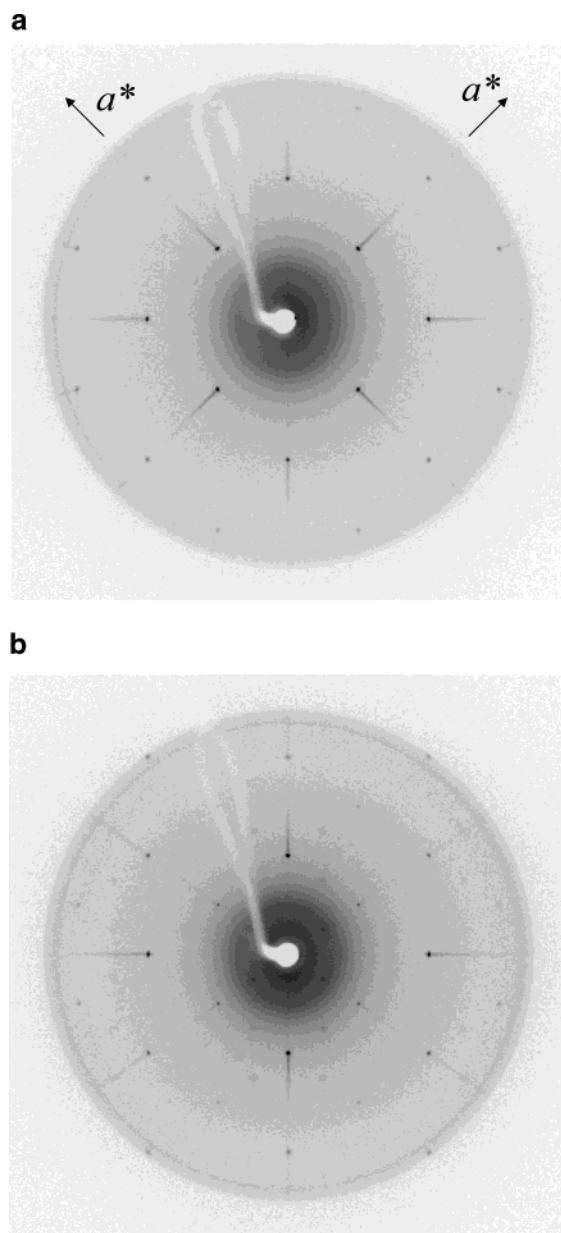


**Figure 6.** (a)  $\{hk0\}^*$  and (b)  $\{hh1\}^*$  precession photographs of electrochemically delithiated cubic  $\text{Li}_x\text{MnO}_2$  single crystal. MoK $\alpha$  radiation filtered by Zr foil was used.

atom	<i>x</i>	<i>y</i>	<i>z</i>	$U_{\text{eq.}} (\text{\AA}^2)$	sof
Mn	0	0	0	0.014(2)	0.48(3)
O	1/2	1/2	1/2	0.033(5)	1

suggesting Li atoms. The final atomic coordinates and displacement parameters are given in Table 4. The refined occupancy parameter for Mn, the value of which is 48%, is well consistent with the chemical analysis. The derived Mn–O distance of 2.048(2)  $\text{\AA}$  is longer than that expected for  $\text{Mn}^{4+}$ . However this can be explained by about 50% vacancy of the Mn site.

Figure 8 compares the X-ray powder diffraction patterns of as-grown orthorhombic  $\text{LiMnO}_2$  crystals and the chemically delithiated  $\text{Li}_x\text{MnO}_2$  crystals. The cubic lattice parameter of  $\text{Li}_x\text{MnO}_2$ , determined by a least-squares refinement using the powder data, was  $a = 4.088(6) \text{\AA}$ . As in the present single-crystal X-ray study, the (111) peak of the cubic spinel structure at around

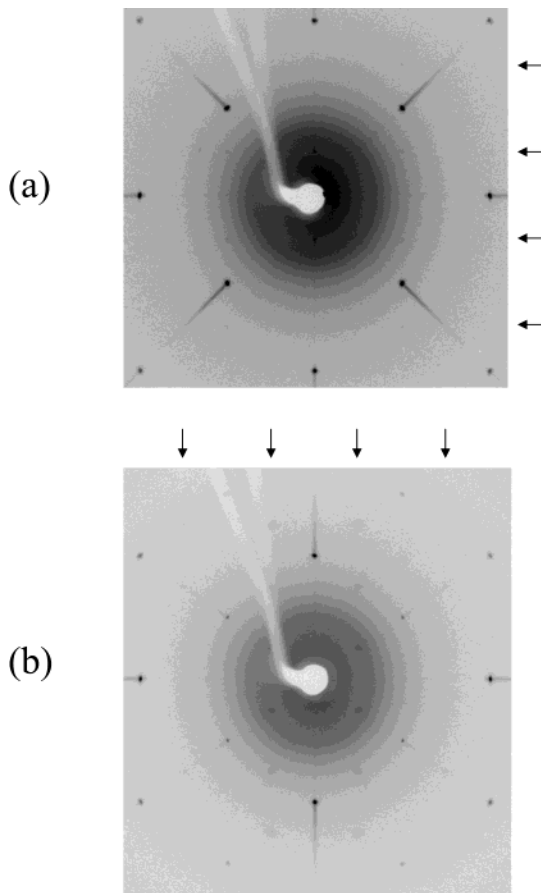


**Figure 7.** Magnified photographs of the center regions of (a)  $\{hk0\}^*$  and (b)  $\{hh1\}^*$  precession photographs shown in Figure 6. Some additional spots indicating the superlattice structure and diffuse scattering are indicated by arrows.

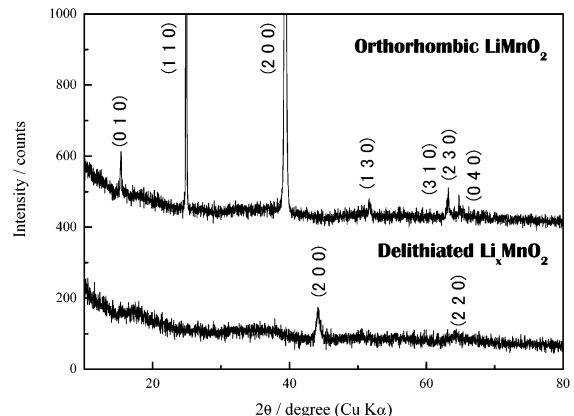


**Figure 8.** X-ray powder diffraction patterns of as-grown  $\text{LiMnO}_2$  single crystals and the chemically delithiated  $\text{Li}_x\text{MnO}_2$  single crystals. The correction for preferred orientation caused by their needlelike crystal shapes was not performed.

19° in  $2\theta$  could not be observed in this pattern. Therefore, the average structure of the chemically delithiated sample also can be described as the disordered rocksalt-type structure.

Magnetic susceptibility was measured as a function of temperature at fixed fields using the chemically delithiated  $\text{Li}_x\text{MnO}_2$  single-crystal samples. Figure 9 shows a typical temperature dependence from 5 to 300 K at 100 Oe. The open and filled marks correspond to measurements on field cooling and on heating after zero-field cooling, respectively. A sharp maximum appears

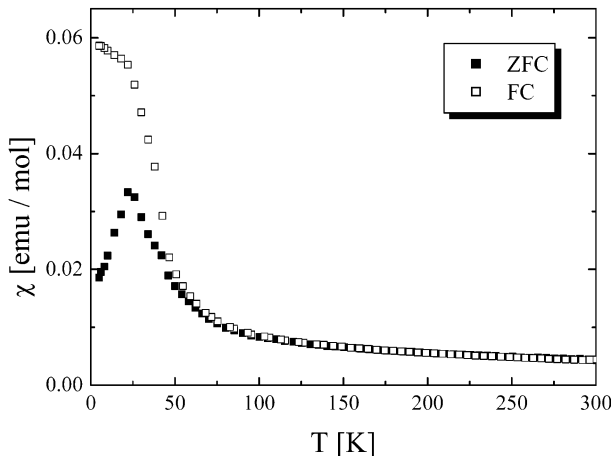


**Figure 9.** Temperature dependence of the magnetic susceptibility for the chemically delithiated  $\text{Li}_x\text{MnO}_2$  single crystals measured at  $H = 100$  Oe after zero-field cooling (filled symbols) and on-field cooling (open symbols).

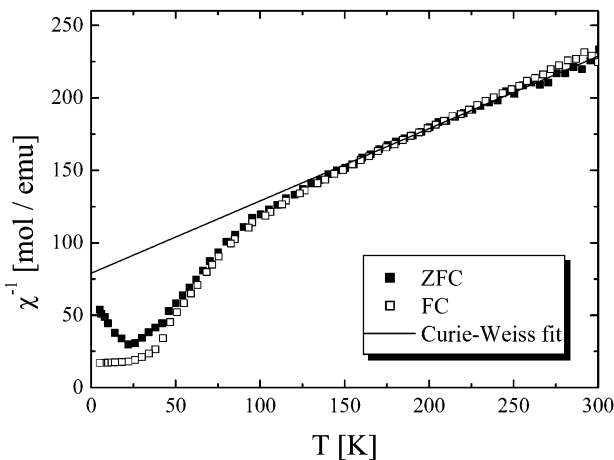


**Figure 10.** Inverse magnetic susceptibility for the chemically delithiated  $\text{Li}_x\text{MnO}_2$  single crystals. The Curie-Weiss fit is indicated.

at 24 K in the ZFC magnetization, and an abrupt increase of the FC magnetization is noticeable with decreasing temperature below 50 K, indicating the presence of a ferromagnetic component. The origin of the ferromagnetic component in  $\text{Li}_x\text{MnO}_2$  is not clear. The complex magnetic behavior may come from the contribution of  $90^\circ \text{ Mn}^{4+}-\text{O}^{2-}-\text{Mn}^{4+}$  ferromagnetic interaction reported by Blasse.<sup>25</sup> However, as ferromagnetism is also observed in the parent  $\text{LiMnO}_2$  (Figure 4),<sup>22</sup> it may be caused by a small amount of magnetic impurity. To confirm this phenomenon, further magnetic properties below 24 K should be measured using higher quality samples.

The inverse susceptibility is plotted in Figure 10, including a Curie-Weiss law fit to the data above 150 K. The extracted Weiss temperature and Curie constant are  $\theta = -158$  K and  $C = 2.00$  emu K/mol, respectively. A negative Weiss temperature indicates antiferromagnetic interaction between  $\text{Mn}^{4+}$  spins. From the Curie constant, the effective moment is determined to be  $\mu_{\text{eff}} = 4.00 \mu_B$ , which is slightly larger than the theoretical spin only value of  $3.87 \mu_B$  for  $\text{Mn}^{4+}$  ( $S = 3/2$ ). This

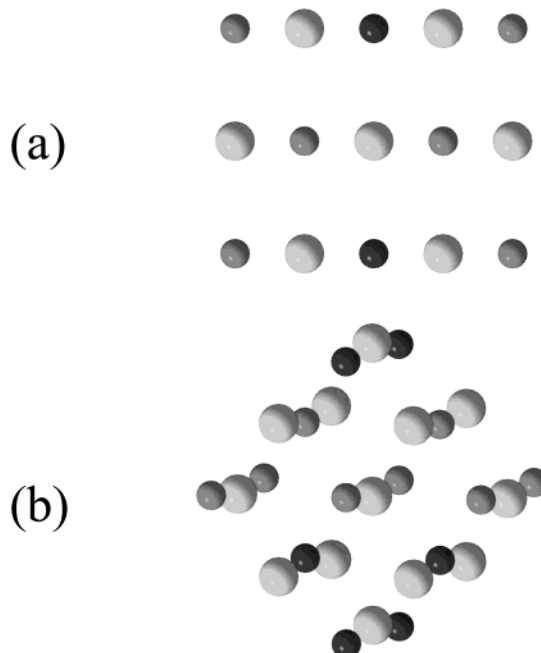


**Figure 11.** Rocksalt-type atomic arrangements in the parent orthorhombic  $\text{LiMnO}_2$  structure, viewed along (a) [010] and (b) [100] directions. The gray, black, and white balls correspond to the Li, Mn, and O atoms, respectively.

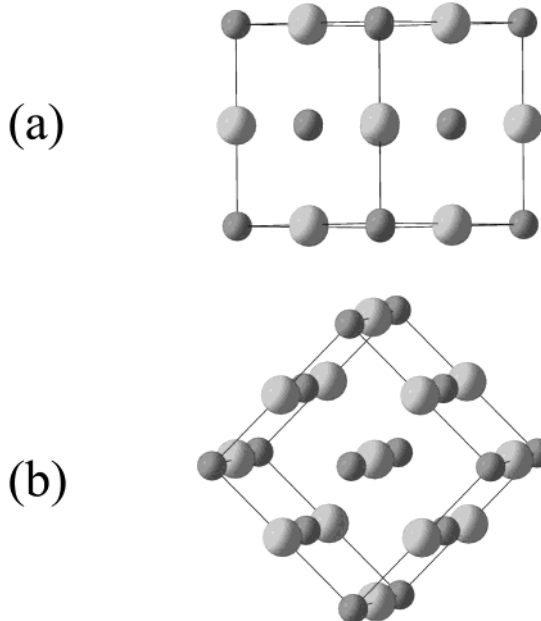


**Figure 12.** Rocksalt-type atomic arrangements in the delithiated cubic  $\text{MnO}_2$  structure, viewed along (a) [110] and (b) [100] directions. The gray and white balls correspond to the Mn and O atoms, respectively.

fact is consistent with the chemical analysis results that show a lithium content of 6%, which implies an equivalent concentration of  $\text{Mn}^{3+}$  ( $S = 2$ ). Previously, Greedan et al. reported  $\mu_{\text{eff}} = 3.97 \mu_B$  for the spinel-type  $\lambda\text{-MnO}_2$  samples prepared by a similar chemical delithiation technique.<sup>24</sup> From these facts, we can be fairly certain that a novel disordered rocksalt-type  $\text{MnO}_2$  can be prepared by delithiation from the parent orthorhombic  $\text{LiMnO}_2$ .

**Structural Transformation Mechanism.** The present single-crystal X-ray diffraction study revealed the structure change together with lithium extraction reaction from the parent orthorhombic zigzag-layered struc-

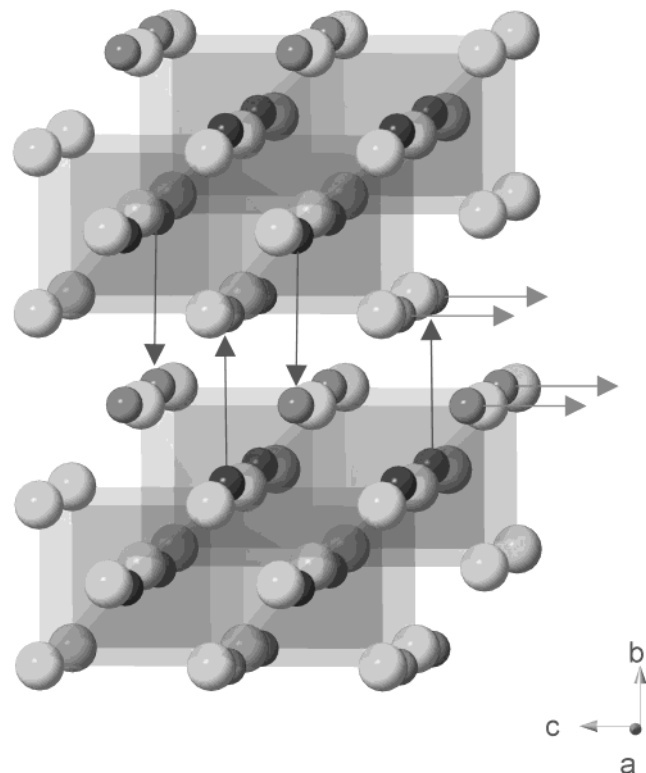


**Figure 13.** Atomic migration model for Li (arrows) and Mn (arrows) atoms from the orthorhombic  $\text{LiMnO}_2$  structure to the cubic rocksalt-type  $\text{MnO}_2$  structure. The balls correspond to the Li, Mn, and O atoms, respectively. The  $\text{MnO}_6$  are drawn with the octahedra. Atomic migration model for Li (gray arrows) and Mn (black arrows) atoms from the orthorhombic  $\text{LiMnO}_2$  structure to the cubic rocksalt-type  $\text{MnO}_2$  structure. The gray, black, and white balls correspond to the Li, Mn, and O atoms, respectively. The  $\text{MnO}_6$  are drawn with the transparent octahedra.

ture to the cubic disordered rocksalt-type one. Because of the characteristic and anisotropic morphology of the starting single-crystal specimen, we have successfully pursued the mechanism of structural transformation by using single-crystal X-ray diffraction photographs.

The parent orthorhombic  $\text{LiMnO}_2$  has a zigzag layered structure, as mentioned above (Figure 1). On the other hand, this structure can be also described as a cubic closest packing for oxygen atoms, in which both of the Li and Mn atoms occupy the octahedral  $\text{O}_6$  interstices. Figure 11 shows the rocksalt-type atomic arrangement in the parent  $\text{LiMnO}_2$  structure. Each view direction in Figure 11(a) and (b) corresponds to the X-ray photographs shown in Figure 3(a) and (b), respectively. Similarly, the ideal rocksalt-type atomic arrays (Figure 12(a) and (b)) correspond to the directions of the X-ray photographs of the electrochemically delithiated single crystal shown in Figure 6(a) and (b), respectively. It should be emphasized that we have taken the X-ray photographs (Figures 3 and 4) from the same direction to the crystal shape (Figures 2 and 5). Namely, the incident directions of X-ray to the characteristic crystal faces in Figure 11(a) and (b) are the same as those in Figure 12(a) and (b), respectively. From these facts, we can easily understand that this structure change is not caused by oxygen rearrangement and has been achieved

by the migration of not only all of the lithium ions but also half of the manganese ions, as summarized in Figure 13. First, all of the  $\text{Li}^+$  migrates out of the lattice by the electrochemical potential, resulting in the formation of vacant octahedral sites (gray arrows in Figure 13). Then, half of the manganese ions migrate statistically into the vacant octahedral sites (black arrows in Figure 13). Accordingly, the migration of metal ions has accompanied a slight shift for oxygen atoms to the ideal CCP positions, resulting in the cubic symmetry. We think that the manganese ion migration could be caused by the structural instability of the “zigzag layered  $\text{MnO}_2$ ”.

## Conclusion

The present single-crystal X-ray diffraction study revealed the structure change together with lithium extraction reaction from the parent orthorhombic zigzag-layered  $\text{LiMnO}_2$  structure to the cubic disordered rock-salt-type  $\text{Li}_x\text{MnO}_2$  with  $x < 0.1$ . The single-crystal to single-crystal transformation has been confirmed by the single-crystal X-ray precession method. The disordered rocksalt-type structure was previously predicted from a viewpoint of crystallographic phase transformation. In the present study, the metastable phase has been obtained as a single-crystal form for the first time.

On the other hand, low-temperature synthetic techniques called “chimie douce” have resulted in major developments in the solid state chemistry of transition metal oxides. The systematic study of oxide bronzes in the period 1950–1980 paved the way to further advances in the solid state chemistry of oxides, including the alkali metal intercalation–deintercalation chemistry by soft chemistry or electrochemical methods. These techniques also gave access to new metastable compounds such as  $\lambda\text{-MnO}_2$ <sup>26</sup> and several new forms of  $\text{TiO}_2$ .<sup>27–29</sup> In the present study, we report a novel disordered rocksalt-type manganese dioxide, prepared by the electrochemical and chemical delithiation from the parent orthorhombic  $\text{LiMnO}_2$ .

It should be noted that it is not clear from the present work whether the rocksalt-type form of  $\text{MnO}_2$  can be stabilized without finite amounts of  $\text{Li}^+$ , as in the case of  $\lambda\text{-MnO}_2$ . The superlattice spots and diffuse scattering observed in the present single-crystal X-ray study may be caused by the remaining lithium ions. Further soft chemical studies for the  $\text{LiMnO}_2$  crystals and polycrystalline samples should be carried out. We believe that the disordered rocksalt-type structure is a key to understanding the good and stable characteristics of the charge–discharge cycles in the  $\text{LiMnO}_2$  electrodes for the battery use.

CM034147B

(26) Hunter, J. C. *J. Solid State Chem.* **1981**, *39*, 142.

(27) Marchand, R.; Brohan, L.; Tournoux, M. *Mater. Res. Bull.* **1980**, *15*, 1129.

(28) Latroche, M.; Brohan, L.; Marchand, R.; Tournoux, M. *J. Solid State Chem.* **1989**, *81*, 78.

(29) Akimoto, J.; Gotoh, Y.; Oosawa, Y.; Nonose, N.; Kumagai, T.; Aoki, K.; Takei, H. *J. Solid State Chem.* **1994**, *113*, 27.